Cloud Publications
International Journal of Advanced Remote Sensing and GIS
2016, Volume 5, Issue 3, pp. 1580-1591
ISSN 2320 - 0243, Crossref: 10.23953/cloud.ijarsg.45

Research Article | Open Access

Assessment of the Spectral Characteristics of Different Physiological Stages of Some Olive cvs and Its Relation with Productivity

Amany F. ELwesemy[1], Nazmy A. Abdelghany[2], Ayman F. Abohadid[2], and Mohamed A. Aboelghar[1]

[1]Agricultural Applications Department, National Authority for Remote Sensing and Space Sciences, Cairo, Egypt
[2]Horticulture Department, Faculty of Agriculture, Ain Shams University, Cairo, Egypt

Publication Date: 5 March 2016

DOI: https://doi.org/10.23953/cloud.ijarsg.45

Abstract Remote sensing satellite imagery is the tool to obtain synoptic, multi-temporal, dynamic and timely efficient information about any target on Earth. The main objective of the current study is to use remote sensing satellite data and field spectral reflectance measurements to identify the spectral pattern of the different cultivars of olives and to statistically correlate this spectral reflectance pattern with crop productivity. The study was carried out in El-Beheira governorate (Wadi El Natrun) city during the whole year of 2014. The three observed varieties were Picual, Manzanillo and Kalamata. Measurements were carried out for five growth stages: dormancy stage, flowering stage, fruit sat stage, mature stage and ripening stage. The spectral reflectance pattern for each cultivar through the different growth stages was identified. Then, seven vegetation indices (normalized difference vegetation index (NDVI), modified chlorophyll absorption ration index (MCARI), triangular vegetation index (TVI), modified chlorophyll absorption ration index-1 (MCARI-1), modified chlorophyll absorption ration index-2 (MCARI-2), modified triangular vegetation index-2 (MTVI2) and chlorophyll index (CI)) were calculated through the five growth stages for each cultivar and then were observed as estimators for crop yield modeling. Analysis of the result based on the comparison of the correlation coefficient (r^2) for all generated models, the target is to identify the optimal vegetation index and the optimal growth stage to predict yield for each variety. Generally, Manzanillo variety showed the highest reflectance followed by Picual and Kalamata. The result showed that the highest (r^2) was with the two cultivars Picual and Kalamata during mature stage, while the highest (r^2) was with cultivar Manzanillo during fruit sat stage. While the lowest (r^2) was found during dormancy stage for the three cultivars.
Keywords *Olive Tree; Spectroradiometer; Spectral Characteristics*

1. Introduction

Olive *(Oleaeuropaea L.)* is one of the most important crops in Egypt. In 2014, Olive in Egypt occupies 82047.63 hectare with a total product of 563070 tons as of 2014. The top olive producers' areas in Egypt are the west coast, the province of Faiyum, Siwa Oasis, northern Sinai and Wadi El Natrun. Because of the importance of Olive cultivation for national economy, there is a high need to facilitate using remote sensing techniques in monitoring and predicting the yield of olive through remotely sensed statistical empirical models.

Remote sensing is the science to detect, measure, record and analyze energy in a selected portion of the electromagnetic spectrum. Remote sensing techniques, in particular, multispectral visible and Infra-Red (IR) reflectance and emission can provide an instantaneous, non-destructive, and quantitative assessment of crops ability to intercept radiation and photosynthesize [1].

There have been a lot of efforts worldwide to employ remote sensing techniques in crop monitoring and crop yield prediction. Most of these works showed that remote sensing technology was encouraging and promising crop yield as a key element for rural development. Statistical model process is based on Vegetation Indices (VI) such as (Normalized Difference Vegetation Index (NDVI), modified chlorophyll absorption ration index (MCARI), triangular vegetation index (TVI), modified chlorophyll absorption ration index-1 (MCARI-1), modified chlorophyll absorption ration index-2 (MCARI-2), modified triangular vegetation index-2 (MTVI2) Chlorophyll Index (CI)). These could be calculated from remote sensing satellite data as well as remotely sensed ground observation tools.

Gong et al. [2; 5] concluded that remote sensing statistical models are chiefly based on using various regressions that compute the crop yield empirically. The explicit and clear description of the mechanism or the effect of each input on crop yield is one of the significant factors of this group of models. Spectral characteristics in the form of vegetation indices could be used with this group of models. Simply, vegetation indices are algebraic combinations of remotely sensed spectral bands that can tell something useful about vegetation. These vegetation indices have proved to be very useful factors for explaining variability of the crop yield, which can be available for use in yield forecasting models. Lately, hyper spectral remote sensing techniques enlarged significantly the applications of remote sensing techniques. Govender et al. [6] Hyperspectral remote sensing imagers acquire many, very narrow, contiguous spectral bands throughout the visible, near-infrared, mid-infrared, and thermal infrared portions of the electromagnetic spectrum. Hyperspectral sensors typically collect 200 or more bands enabling the construction of an almost continuous reflectance spectrum for every pixel in the scene. Contiguous, narrow bandwidths characteristic of hyperspectral data allow for in-depth examination of earth surface features which would otherwise be 'lost' within the relatively coarse bandwidths acquired with multispectral scanners. Maselli et al. [7] extracted olive tree Normalized difference vegetation index (NDVI) values from MODIS imagery and used a modified parametric model (C-fix) and a bio-geochemical model (BIOME-BGC) to enable the prediction of daily olive tree gross primary production and olive tree net primary production (NPP). Guzmán et al. [8] used infrared machine vision system to detect olive fruit quality. Brilli et al. [9] estimated olive (*Oleaeuropaea L.)* gross primary production (GPP) combining ground measurements and multi-sensor satellite data.

Ariana & Lu, [10] used Hyper spectral imaging to detect the defect internal option for pickling, however, the technique still cannot meet the online speed requirement because of the need to acquire and analyze a large amount of image data. Hyper spectral reflectance characteristics was used to discriminate different geographical origins of *Jatropha curcas L.* seeds to estimate chlorophyll content and to detect macronutrients content in oil seeds. Garcia-Maraver et al. [11] used hyperspectral technique to analyze the relation between the cellulose, hemi cellulose and lignin content and the thermal behavior of residual biomass from olive trees.

The main objectives of the current research are to study the spectral properties of the three cultivars of olive leaf during the whole season 2014 and determine the best spectral bands to separate the olive plantations as well as study aims to link crop productivity by spectral reflectance, research is a first step towards limiting the cultivation of olives at the State level. The objective of this study is Field spectral measurements and identifies the spectral signature of the different cultivars of olives, linking productivity of the olive crop with different spectral characteristics.

2. Materials and Methods

The study was carried out in olive farm located in Wadi El Natrun area, El-Beheira governorate between longitudes 30°14'37.43" and 30°14'58.07"E and latitudes 30°19'54.69" and 30°19'43.57"N. The Farm covers about 12.6 hectare where shown in Figure 1. The soil of the farm is Sandy clay and ratio of Calcium carbonate is 10%.

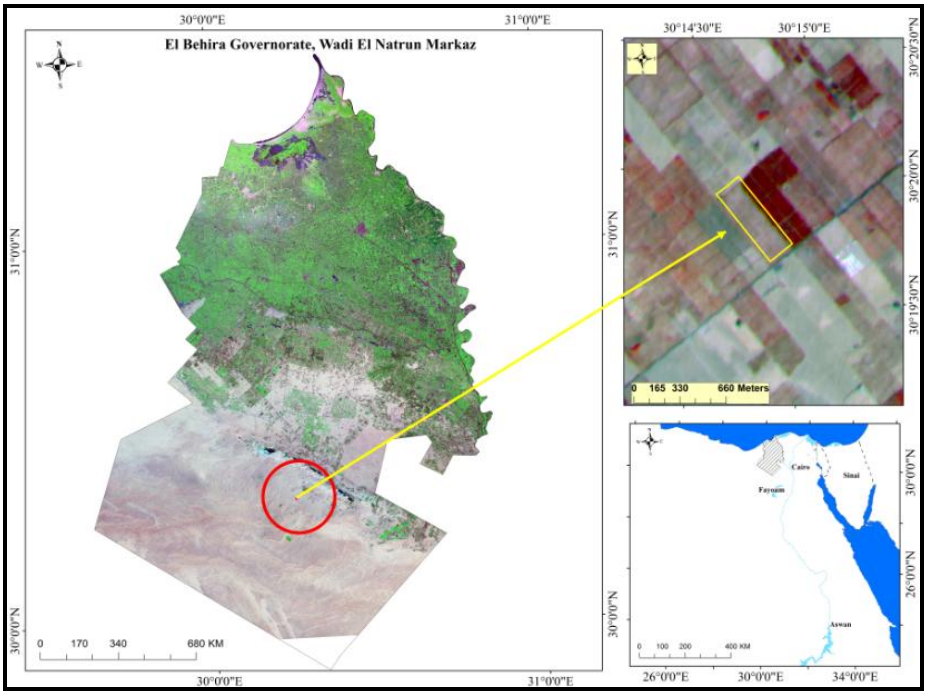

Figure 1: *Field Experiment Location*

Land surface temperature in the study area ranged from 5 to 15 Celsius degree in January and increased gradually to range from 28 to 38 Celsius degree in August as shown in Figure 2.

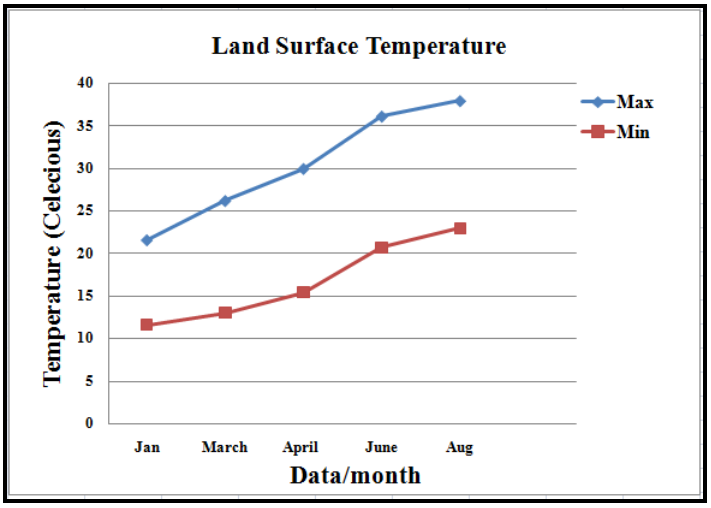

Figure 2: *Mean Maximum & Minimum Land surface Temperature of Study Area*

Analytical field spectroradiometer (ASD Field Spec) was used to measure the reflection of the different olive trees under investigation. Data were collected on cloudless days from 10 am clock to 2 pm in order to minimize the atmospheric effects. Measurements were carried out in a full optical spectral range (Visible – Near Infrared – Short Wave Infrared) starting from 350 nm to 2500 nanometer (nm). The sampling interval is 1.4 nm at the spectral range (350-1050 nm) while it is 2 nm at the spectral range (1000-2500 nm). These are the intervals which the device is capturing the reflectance. The device automatically performs an interpolation for the data and gives the final data output with (1 nm) interval for the all spectrum range (350-2500 nm). The spectrum characteristics of the device are shown in Table 1. The protocol used for the collection of spectral data is based on measuring radiance from a Spectralon® panel. A designed probe was attached to the instrument's fiber-optic cable to be used to ensure standardized environmental conditions for reflectance measurement. The fiber-optic cable provides the flexibility to adapt the instrument to a wide range of applications. Bare fore optic 25 degrees used for outdoor measurements resulting circular field of view with 3 cm diameter as measurements were taken at 5 cm height in nadir position (90 degrees) over the measured plants. In the current study, the measurements were performed by holding the pistol grip by hand. As recommended in the instructions of using the device, the Spectralon® was tilted directly towards the sun during optimization.

Table 1: *The ASD Field Spec 3 Specifications*

Spectral Range	350 - 2500 nm
Spectral Resolution	3 nm at 700 nm and 8.5 nm @ 1400 nm and 6.5 nm @ 2100 nm.
Sampling Interval	1.377 nm for 350 - 1000 nm and 2 nm for 1000 - 2500 nm

The farm was divided into five spots, each spot contains twelve olive trees belong to the three observed cultivars. Each growing stage was covered by sixty (60) hyper spectral measurements with a total of three hundred (300) measurements overall the whole year of 2014. Table 2 shows the scheduled time for the field measurements while Figure 3 shows the location of measurements within the location.

Table 2: *Scheduled Time for Field Measurements*

Stage	Time
Dormancy Stage	20/1/2014
Flowering Stage	10/3/2014
Fruit Sat Stage	28/4/2014
Mature Stage	9/6/2014
Ripening Stage	13/8/2014

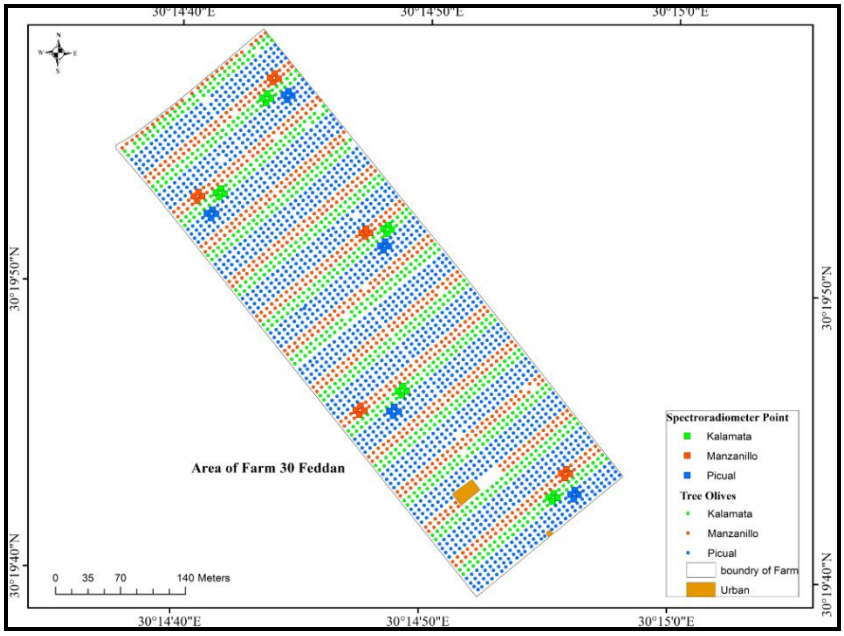

Figure 3: *Location of the Measurements*

As the first step of the analysis, spectral reflectance pattern for each cultivar in each growing stage was identified and compared. Seven vegetation indices were calculated to be tested as estimators for crop yield. Finally, accuracy assessment was carried out to identify the optimal vegetation index and the optimal growing stage to predict crop yield for each cultivar. Equations that were used to calculate the different indices and the references for each index are explained in Table 3.

Table 3: *The Used Vegetation Indices (VIs)*

VIS	Equation	Reference
NDVI	$\frac{(R800 - R670)}{(R800 + R670)}$	Rouse et al. [12]
MCARI	$[(R700 - R670) - 0.2(R700 - R550)] * \left(\frac{R700}{670}\right)$	Daughtry et al. [13]
TVI	0.5[120(R750-R550)-200(R670-R550)]	Broge & Leblanc [14]
MCARI1	1.2[2.5(R800-R670)-1.3(R800-R550)]	Haboudane et al. [15]
MCARI2	$\frac{1.5[2.5(R800 - R670) - 1.3(R800 - R550)]}{\sqrt{(2R800 + 1)^2 - (6R800 - 5\sqrt{R670}) - 0.5}}$	Haboudane et al. [15]

MTVI2	$\frac{1.5[1.2(R800-R500)-2.5(R670-R550)]}{\sqrt{(2R800+1)^2-(6R800-5\sqrt{R670})-0.5}}$	Haboudane et al. [15]
Chlorophyll index	$\frac{R750}{(R700+R710)-1}$	Gitelson et al. [16]

For modeling process, descriptive statistics were applied to characterize the parameters of continuous environmental variables such as mean, median, standard deviation, minimum and maximum. Were imported to the Statistical Package of the Social Sciences (SPSS) version 18 statistical software for descriptive statistical analysis? We made relationships between the dependent (yield) (Kg) and independent (vegetation indices biophysical parameters) variables involved in the simple regression analysis.

The stepwise simple linear regression method was used to model Normalized difference vegetation index (NDVI), Modified chlorophyll absorption ratio index (MCARI), Triangular vegetation index (TVI), Modified chlorophyll absorption ratio index 1 (MCARI1), Modified chlorophyll absorption ratio index 2 (MCARI2), Modified triangular vegetation index (MTVI2), Chlorophyll index and grain yield predictions. To avoid the danger of too many parameters being included, the stepwise Forward method was used. The production function: or Grain Yield = f (vegetation indices biophysical parameters).

$$Y=a+ b*x \qquad \text{(Linear regression model)}$$

Where, Y is the actual grain yield and X are VIS. A is intercept, b is the regression coefficients. The final regression equation was derived through a researcher controlled trial, error approach and the impact of grain yield constraints on grain yield. Two main assumptions were used to check the relationships between the dependent (grain yield) and independent (vegetation indices biophysical parameters) variables involved in the simple regression analysis.

Regression analysis also has an assumption of linearity. The relationship between the dependent variable and the independent variables for a linear relationship was tested and was the basis of the correlation of the variables [17]. The relationship between predict and the predictors is linear. The simple linear regression models were applied to linear relationships. The linearity between grain yield and vegetation indices biophysical parameters was done using SPSS 18.

The square of the correlation coefficient (R^2) was computed to measure the goodness-of-fit of the model. It takes values between 0 (the points are completely random) and 1 (all the points lie exactly on the regression line). (R^2) describes the proportion of the total variability of grain yield (Y) which is explained by the linear relationship of Y on the entire vegetation indices biophysical parameters , and gives an indication of the goodness-of-fit of a model .However, every time another independent variable is added, the value (R^2) of is necessarily increased.

Three spectral regions of Spectroradiometer data (Visible, near infra-red and Shortwave infra-red) and seven spectral vegetation indices (NDVI, MCARI, TVI, MCARI1, MCARI2, MTVI2 and Chlorophyll Index) were used in the modeling process with crop yield. All generated models were validated using the correlation coefficient between the actual and predicted yields (r^2).

3. Results and Discussion

3.1. Analysis of Spectral Reflectance Characteristics

Spectral reflectance of plant leaves is characterized and uniquely identified by very low spectral reflectance in the red band followed by high spectral reflectance in near infra-red band and low spectral reflectance in the shortwave infra-red. Near infra-red band usually shows the highest reflectance value while visible bands show the lowest ones. The spectral zones for the three cvs showed that the highest spectral reflectance was in near infra-red infrared spectral zone (700–1300 nm), relatively low reflectance in the spectral zone (1450–1800 nm) whiles the lower reflectance was found in the spectral zone (1950-2300 nm). The lowest reflectance was found in the spectral zone (350-650).

Analysis of the spectral reflectance characteristics for each growing stage showed that in the dormancy stage, in visible bands Kalamata cultivar showed the highest spectral reflectance followed by Picual when Manzanillo cultivar showed the lowest spectral reflectance. In near infra-red bands, Kalamata cultivar showed the highest reflectance while Manzanillo cultivar was the lowest. Kalamata cultivar showed also the highest reflectance in short wave infrared (AWIR-1 and SWIR-2) while Manzanillo cultivar showed the lowest reflectance. Spectral reflectance pattern for the three cultivars in the dormancy stage is shown in Figure 4.

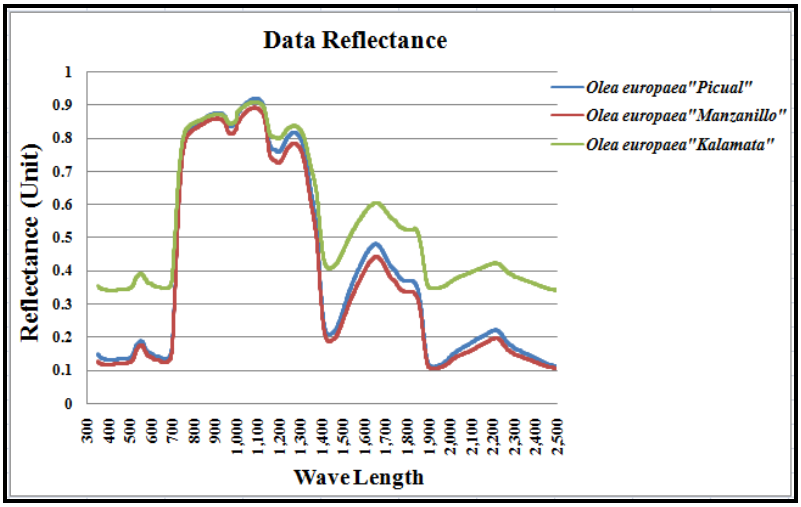

Figure 4: *Spectral Reflectance in All Cultivar in Dormancy Stage*

In flowering stage, Kalamata cultivar showed the highest spectral reflectance in all bands. In near infra-red band, Picual showed the lowest reflectance, however, no significant difference was found in the reflectance of Picual and Manzanillo in visible bands as shown in Figure 5.

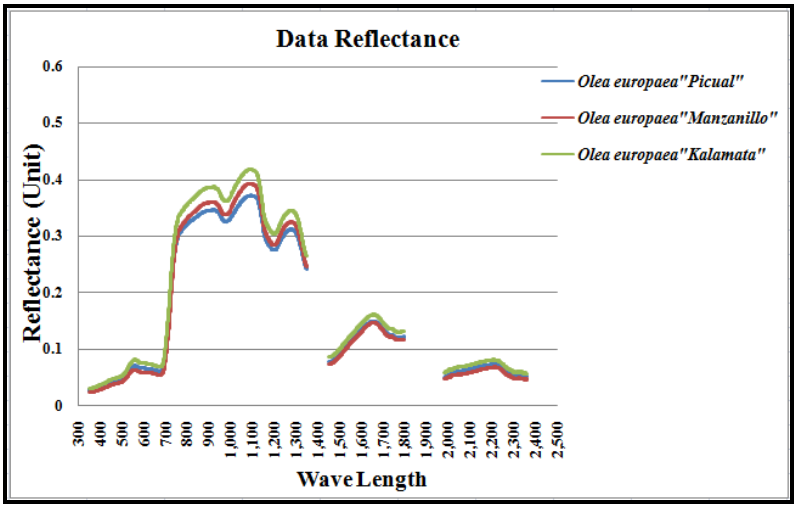

Figure 5: *Spectral Reflectance in All Cultivar in Flowering Stage*

In fruit sat stage, Manzanillo cultivar showed is highest spectral reflectance with while Kalamata cultivar showed the lowest reflectance as shown in Figure 6.

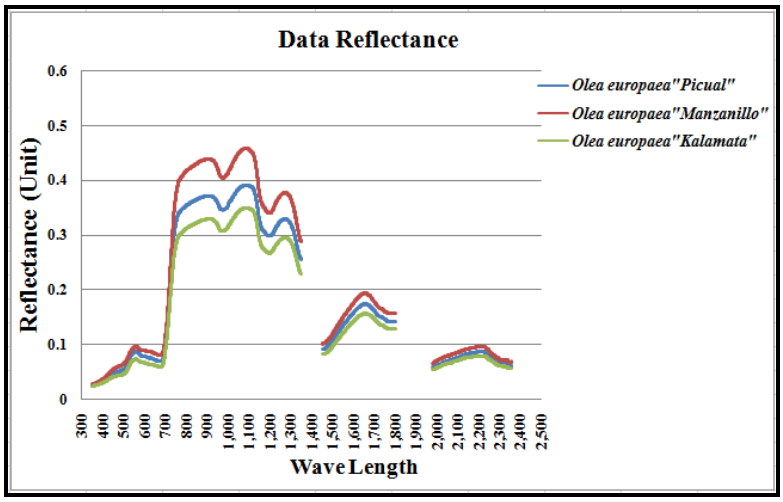

Figure 6: *Spectral Reflectance in All Cultivar in Fruit Sat Stage*

In mature stage, Manzanillo cultivar showed the highest spectral reflectance in all bands followed by Picual cultivar in near infrared and shortwave infrared. No significant difference in the reflectance of the three cultivars in visible spectral region as shown in Figure 7.

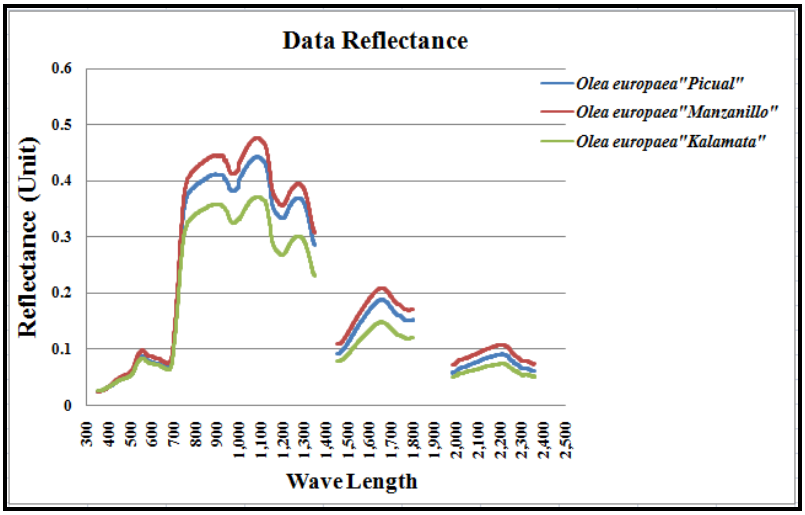

Figure 7: *Spectral Reflectance in All Cultivar in Mature Stage*

In ripening stage, Kalamata cultivar showed the highest reflectance in visible region while Manzanillo showed the lowest reflectance. Manzanillo showed the highest reflectance in near infra-red spectral region while Picual showed the lowest reflectance. In (SWIR-1 and SWIR-2), Kalamata cultivar showed the highest spectral followed by the other two cultivars that gave almost the same reflectance as shown in Figure 8.

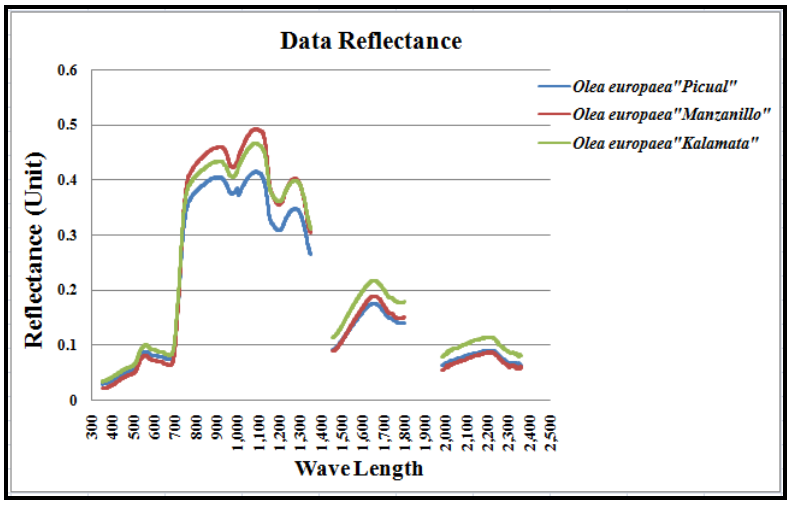

Figure 8: *Spectral Reflectance in All Cultivar in Mature Stage*

3.2. Yield Prediction Modeling

Modeling process in the current study is focusing on statistical empirical models that are limited to the conditions of the experiment. Data for the whole season of 2014 were used in the current study. Three hundred (300) spectral measurements (one hundred for each cultivar) were considered in the modeling process. Vegetation indices (VIs) and yield data were the main inputs in the modeling process. As the first step, each individual factor was used in a simple regression analysis to estimate Olive yield.

Total of Fifteen models were produced, yield prediction for each cultivar was estimated using the data from the five growing stages. It was found that the highest correlation coefficient for the two cultivars

Kalamata and Picual was presented in mature stage (Tables 4 and 5) while the highest correlation coefficient for Manzanillo cultivar was found during fruit sat stage (Table 6). The lowest correlation coefficient for all cultivars was found in dormancy stage. Table 7 showed the highly accurate model for each cultivar.

Table 4: *Simple Regression Models for Picual Yield Prediction in Mature Stage*

Input factor	Intercept(a)	Slope Coefficient (b)	Generated Model	Correlation Coefficient (R^2)
NDVI	-274.008	473.422	Y=-274.008+473.422*NDVI	0.851
MCARI	7.065	975.649	Y=7.065+975.649*MCARI	0.981
TVI	-45.614	5.810	Y=-45.614+5.810*TVI	0.779
MCARI1	-51.494	223.087	Y=-51.494+223.087*MCARI1	0.779
MCARI2	-51.364	57.304	Y=-51.364+57.304*MCARI2	0.774
MTVI2	-23.839	68.901	Y=-23.839+68.901*MTVI2	0.769
Chlorophyll index	27.078	81.214	Y=27.078+81.214*Chlorophyll Index	0.827

Table 5: *Simple Regression Models for Kalamata Yield Prediction in Mature Stage*

Input factor	Intercept(a)	Slope coefficient (b)	Generated model	Correlation coefficient (R^2)
NDVI	-98.902	239.018	Y=-98.902+239.018*NDVI	0.862
MCARI	13.771	985.786	Y=13.771+985.786*MCARI	0.941
TVI	-10.977	4.928	Y=-10.977+4.928*TVI	0.752
MCARI1	-12.268	180.619	Y=-12.268+180.619*MCARI1	0.748
MCARI2	-10.232	45.840	Y=-10.232+45.840*MCARI2	0.787
MTVI2	10.881	55.394	Y=10.881+55.394*MTVI2	0.777
Chlorophyll index	39.973	68.333	Y=39.973+68.333*Chlorophyll Index	0.824

Table 6: *Simple Regression Models for Manzanillo Yield Prediction in Fruit Sat Stage*

Input Factor	Intercept(A)	Slope Coefficient (b)	Generated Model	Correlation Coefficient (R^2)
NDVI	260.482	449.042	Y=-260.482+449.042*NDVI	0.969
MCARI	-40.140	1975.960	Y=-40.140+1975.960*MCARI	0.894
TVI	-242.221	15.755	Y=-242.221+15.755*TVI	0.877
MCARI1	-271.964	622.285	Y=-271.964+622.285*MCARI1	0.779
MCARI2	-291.462	168.073	Y=-291.462+168.073*MCARI2	0.744
MTVI2	-183.170	182.507	Y=-183.170+182.507*MTVI2	0.777
Chlorophyll index	-24.488	177.067	Y=-24.488+177.067*Chlorophyll Index	0.903

Table 7: *Showed the Highest R^2 to Every Cultivar*

Cultivar	Intercept(A)	Slope Coefficient (B)	Generated Model	Correlation Coefficient (R^2)
Picual	7.065	975.649	Y=7.065+975.649*MCARI	0.981
Manzanillo	-260.482	449.042	Y=-260.482+449.042*NDVI	0.969
Kalamata	13.771	985.786	Y=13.771+985.786*MCARI	0.941

According to the presented results, mature and fruit sat are the optimal growing stages for olive monitoring and yield prediction. At the same time, dormancy stage did not show sufficiency in either monitoring crop or predicting the yield. Most of vegetation indices showed high efficiency as estimators for crop yield, however, (MACARI - yield) and (NDVI - yield) models were the highly accurate models for yield prediction. These results agreed with Noureldin et al. [18] and Aboelghar et al. [19].

4. Conclusions

The main objective of the current study is to use hyperspectral remotely sensed data to identify the spectral signature of the different olive cultivars and to link productivity of the olive crop with different hyperspectral vegetation indices that were calculated from spectral characteristics to predict olive yield. The study was carried out in an observation site in Wadi El-Natrun city using the dataset from season 2014.

Seven vegetation indices were tested in the current study: normalized difference vegetation index (NDVI), modified chlorophyll absorption ratio index (MCARI), triangular vegetation index (TVI), modified chlorophyll absorption ratio index 1 (MCARI1), modified chlorophyll absorption ratio index 2 (MCARI2), modified triangular vegetation index (MTVI2) and Chlorophyll index. Molding and validation process were carried out for each cultivar. The most accurate models were generated during mature stage in the case of the two cultivars Picual and Kalamata and in fruit sat stage in the case of Manzanillo cultivar. The lowest accuracy was found during dormancy stage with all cultivars.

References

[1] Ahamed, T., Tian, L., Zhang, Y., and Ting, K.C. *A Review of Remote Sensing Methods for Biomass Feedstock Production.* Biomass and Bioenergy. 2011. 35 (7) 2455-2469.

[2] Gong, P., Pu, R., Biging, G.S., and Larrieu, M.R. *Estimation of Forest Leaf Area Index Using Vegetation Indices Derived from Hyperion Hyperspectral Data.* IEEE Transactions on Geosciences and Remote Sensing. 2003. 41 (6) 1355-1362.

[3] Guréif, M., and Duke, C.L. *Adjustment Procedures of a Crop Model to the Site Specific Characteristics of Soil and Crop Using Remote Sensing Data Assimilation.* Agriculture, Ecosystems and Environment. 2000. 81; 57-69.

[4] Hamar, D., Ferncz, C., Lichtenberger, J., Tarcsai, G., and Ferncz, A. *Yield Estimation for Corn and Wheat in the Hungarian Great Plain Using Landsat MSS Data.* International Journal of Remote Sensing. 1996. 17; 1689-1699.

[5] Walthall, C., Dulaney, W., Anderson, M., Norman, J., Fang, H., and Liang, S. *A Comparison of Empirical and Neural Network Approaches for Estimating Corn and Soybeans Leaf Area Index from Landsat ETM_ Imagery.* Remote Sensing of Environment. 2004. 92; 465-474.

[6] Govender, M., Chetty, K., and Bulcock, H. *A Review of Hyperspectral Remote Sensing and Its Application in Vegetation and Water Resource Studies.* Water Sa. 2007. 33 (2) 145-151.

[7] Maselli, F., Chiesi, M., Brilli, L., and Moriondo, M. *Simulation of Olive Fruit Yield in Tuscany through the Integration of Remote Sensing and Ground Data.* Ecological Modelling. 2012. 244; 1-12.

[8] Guzmán, E., Baeten, V., Pierna, J.A.F., and García-Mesa, J.A. *Infrared Machine Vision System for the Automatic Detection of Olive Fruit Quality.* Talanta. 2013. 116; 894-898.

[9] Brilli, L., Chiesi, M., Maselli, F., Moriondo, M., Gioli, B., Toscano, P., and Bindi, M. *Simulation of Olive Grove Gross Primary Production by the Combination of Ground and Multi-Sensor Satellite Data.* International Journal of Applied Earth Observation and Geoinformation. 2013. 23; 29-36.

[10] Ariana, D.P., and Lu, R. *Hyperspectral Waveband Selection for Internal Defect Detection of Pickling Cucumbers and Whole Pickles.* Computers and Electronics in Agriculture. 2010. 74 (1) 137-144.

[11] Garcia-Maraver, A., Salvachúa, D., Martínez, M.J., Diaz, L.F., and Zamorano, M. *Analysis of the Relation between the Cellulose, Hemicellulose and Lignin Content and the Thermal Behavior of Residual Biomass from Olive Trees.* Waste Management. 2013. 33 (11) 2245-2249.

[12] Rouse, J.W., Haas, R.H., Schell, J.A., Deering, D.W., and Harlan, J.C., 1974: *Monitoring the Vernal Advancements and Retrogradation of Natural Vegetation.* NASA/GSFC, Final Report, Greenbelt, MD, USA. 1-137.

[13] Daughtry, C.S.T., Walthall, C.L., Kim, M.S., Brown de Colstoun, E., and McMurtrey, J.E., III. *Estimating Corn Leaf Chlorophyll Concentration from Leaf and Canopy Reflectance.* Remote Sensing of Environment. 2000. 74; 229-239.

[14] Broge, N.H., and Leblanc, E. *Comparing Prediction Power and Stability of Broadband and Hyperspectral Vegetation Indices for Estimation of Green Leaf Area Index and Canopy Chlorophyll Density.* Remote Sensing of Environment. 2000. 76; 156-172.

[15] Haboudane, D., Miller, J.R., Pattey, E., Zarco-Tejada, P.J., and Stachan, I.B. *Hyperspectral Vegetation Indices and Novel Algorithms for Predicting Green LAI of Crop Canopies: Modeling and Validation in the Context of Precision Agriculture.* Remote Sensing of Environment. 2004. 90; 337-352.

[16] Gitelson, A.A., Viña, A., Ciganda, C., Rundquist, D.C., and Arkebauer, T.J. *Remote Estimation of Canopy Chlorophyll Content in Crops.* Geophysical Research Letters. 2005. 32; L08403.

[17] Ostrom, C.W., 1990: *Time Series Analysis and Regression Techniques*. Second Edition, Quantitative Applications in the Social Sciences, V. 07-009: Newbury Park: SAGE Publications, Inc. 95.

[18] Noureldin, N.A., Aboelghar, M.A., Saudy, H.S., and Ali, A.M. *Rice Yield Forecasting Models Using Satellite Imagery in Egypt.* The Egyptian Journal of Remote Sensing and Space Science. 2013. 16 (1) 125-131.

[19] Aboelghar, M., Ali, A.R., and Arafat, S. *Spectral Wheat Yield Prediction Modeling Using SPOT Satellite Imagery and Leaf Area Index.* Arabian Journal of Geosciences. 2014. 7 (2) 465-474.